

Measurement of large discontinuities using single white light interferogram

Paul Kumar Upputuri,^{1*} Li Gong,² Haifeng Wang,² Manojit Pramanik,¹
Krishna Mohan Nandigana,³ and Mahendra Prasad Kothiyal³

¹School of Chemical and Biomedical Engineering, Nanyang Technological University 637457, Singapore

²Department of Physics, Faculty of Science, National University of Singapore 117542, Singapore

³Department of Physics, Indian Institute of Technology Madras, Chennai 600036, India

*pupputuri@ntu.edu.sg

Abstract: White light interferometry is a widely used tool to extend the unambiguous measurement range of a monochromatic interferometer. In this work, we discuss Hilbert transformation analysis of a single white light interferogram acquired with a single-chip color CCD camera for step height measurement which lies beyond the unambiguous range of the monochromatic interferometry. The color interferogram is decomposed and phase maps for red, green, and blue components are calculated independently using Hilbert transformation. This procedure makes the measurement faster, simpler, and cost-effective. The usefulness of the technique is demonstrated on micro-sample.

©2014 Optical Society of America

OCIS codes: (120.3180) Interferometry; (120.3940) Metrology; (120.2650) Fringe analysis; (120.5050) Phase measurement.

References and links

1. E. Wolf, *Progress in Optics* (Elsevier, 1988), vol. XXVI, pp. 349–393.
2. D. Malacara, *Optical Shop Testing* (John Wiley & Sons Inc, 1992), vol. II, pp. 501–598.
3. L. Yang and P. Colbourne, “Digital laser micro-interferometer and its applications,” *Opt. Eng.* **42**(5), 1417–1426 (2003).
4. N. Krishna Mohan and P. K. Rastogi, “Recent developments in Interferometry for Microsystems Metrology,” *Opt. Lasers Eng.* **47**(2), 199–202 (2009).
5. W. Osten, *Optical inspection of Microsystems* (Florida, CRC Press, 2007).
6. J. C. Wyant and K. Creath, “Advances in interferometric optical profiling,” *Int. J. Mach. Tools Manuf.* **32**(1-2), 5–10 (1992).
7. C. Polhemus, “Two-wavelength interferometry,” *Appl. Opt.* **12**(9), 2071–2074 (1973).
8. K. Creath, “Step height measurement using two-wavelength phase-shifting interferometry,” *Appl. Opt.* **26**(14), 2810–2816 (1987).
9. J. Schmit and P. Hariharan, “Two-wavelength interferometry profilometry with a phase-step error - compensating algorithm,” *Opt. Eng.* **45**(11), 115602 (2006).
10. Y. Y. Cheng and J. C. Wyant, “Multiple-wavelength phase-shifting interferometry,” *Appl. Opt.* **24**(6), 804–807 (1985).
11. U. Paul Kumar, B. Bhaduri, N. Krishna Mohan, and M. P. Kothiyal, “Two wavelength interferometry for 3-D surface profiling,” *Opt. Lasers Eng.* **47**(2), 223–229 (2009).
12. U. Paul Kumar, N. Krishna Mohan, and M. P. Kothiyal, “Measurement of discontinuous surfaces using multiple-wavelength interferometry,” *Opt. Eng.* **48**(7), 073603 (2009).
13. U. Paul Kumar, N. Krishna Mohan, and M. P. Kothiyal, “Multiple wavelength interferometry for surface profiling,” *Proc. SPIE* **7063**, 70630W (2008).
14. P. de Groot and L. Deck, “Surface profiling by analysis of white-light interferograms in the spatial frequency domain,” *J. Mod. Opt.* **42**(2), 389–401 (1995).
15. P. de Groot and L. Deck, “Three-dimensional imaging by sub-Nyquist sampling of white-light interferograms,” *Opt. Lett.* **18**(17), 1462–1464 (1993).
16. P. Sandoz, G. Tribillon, and H. Perrin, “High resolution profilometry by using phase calculation algorithms for spectroscopic analysis of white light interferograms,” *J. Mod. Opt.* **43**(4), 701–708 (1996).
17. S. K. Debnath and M. P. Kothiyal, “Experimental study of the phase-shift miscalibration error in phase-shifting interferometry: use of a spectrally resolved white-light interferometer,” *Appl. Opt.* **46**(22), 5103–5109 (2007).
18. A. Pfortner and J. Schwider, “Red-green-blue interferometer for the metrology of discontinuous structures,” *Appl. Opt.* **42**(4), 667–673 (2003).

19. U. Paul Kumar, W. Haifeng, N. Krishna Mohan, and M. P. Kothiyal, "White light Interferometry for surface profiling with colour CCD," *Opt. Lasers Eng.* **50**(8), 1084–1088 (2012).
20. D. S. Mehta and V. Srivastava, "Quantitative phase imaging of human red blood cells using phase-shifting white light interference microscopy with colour fringe analysis," *Appl. Phys. Lett.* **101**(20), 203701 (2012).
21. L. H. Stefan, *Hilbert Transforms in Signal Processing* (Artech House Inc, 1996).
22. V. D. Madjarova, H. Kadono, and S. Toyooka, "Dynamic electronic speckle pattern interferometry (DESPI) phase analyses with temporal Hilbert transform," *Opt. Express* **11**(6), 617–623 (2003).
23. U. P. Kumar, N. K. Mohan, and M. P. Kothiyal, "Time average vibration fringe analysis using Hilbert transformation," *Appl. Opt.* **49**(30), 5777–5786 (2010).
24. U. Paul Kumar, N. Krishna Mohan, and M. P. Kothiyal, "Characterization of micro-lenses based on single interferogram analysis using Hilbert transformation," *Opt. Commun.* **284**(21), 5084–5092 (2011).
25. K. G. Larkin, D. J. Bone, and M. A. Oldfield, "Natural demodulation of two-dimensional fringe patterns. I. General background of the spiral phase quadrature transform," *J. Opt. Soc. Am. A* **18**(8), 1862–1870 (2001).
26. J. T. Mercado and A. V. Khomenko, "Precision and sensitivity optimization for white light interferometric fiber-optic sensors," *J. Lightwave Technol.* **19**(1), 70–74 (2001).
27. S. K. Debnath, M. P. Kothiyal, and S. W. Kim, "Evaluation of spectral phase in spectrally resolved white-light interferometry: Comparative study of single-frame techniques," *Opt. Lasers Eng.* **47**(11), 1125–1130 (2009).

1. Introduction

The single wavelength phase shifting interferometry (SWPSI) offers excellent vertical resolution and sensitivity [1–6]. It requires more than three phase shifted frames for phase calculation. A serious limitation of single wavelength interferometry is that the unambiguous range is limited to half a wavelength. The approaches adopted to overcome the problem of small dynamic range are based on multiple-wavelength [7–13] and white light interferometry [14–19]. Multiple wavelength technique requires typically 2 or 3 laser wavelengths for surface profiling. White light interferometry is a state-of-the-art technique for measuring discontinuous surface profiles. This makes use of the short coherence length of the white light source. High contrast fringe occurs only when the optical path difference (OPD) is close to zero. The 3-D plot of the axial positions of the zero OPD along the optical axis represents the surface profile of the object under test. Compared to single wavelength phase shifting interferometry, the white light interferometry is rather slow, as the number of frames to be recorded and evaluated is large. The spectrally resolved white light interferometry [16,17], on the other hand gives only a line profile of the object, although the requirement on number of frames is similar to the single wavelength phase shifting interferometry.

Phase shifting white light interferometry (PSWLI) combined with a 3-chip colour CCD camera can make the data acquisition as simple as in single wavelength case [18]. Use of single chip colour CCD has also been demonstrated for this [19,20]. In a 3-chip CCD each chip registers a different primary colour, red (R), green (G), or blue (B). Thus one pixel for chip is used to reproduce image. In a single-chip CCD camera, on the other hand, a group of three pixels is required to register all the three colours of the image with the help of colour filters. A 3-chip colour CCD can give high resolution, but is costly. However, this technique requires typically 5 to 8 phase shifted frames for phase evaluation [18–20]. Though PSI can provide high resolution phase profile; it is time consuming and cannot be used for dynamic measurements. So, fringe analysis using a single frame obviously is an attractive scheme as it makes the measurement faster. Hilbert Transform (HT) method has been successfully applied for single frame analysis [21–25]. The HT method can be applied to a wide range of interferometric measurements. The method has simplicity in the calculation algorithms, and it has relatively shorter calculation time compared to Fourier transform (FT) method. And also the application of HT can be made fully automatic [22].

In this work, we discuss Hilbert transform fringe analysis of a single white light interferogram acquired with a single-chip colour CCD camera for large step-height measurement. First the individual interference data for red, green, blue colors are separated from the color white light interferogram and then processed independently for phase calculation using Hilbert transformation. The present technique does not require phase shifting method, multiple-wavelength laser sources, or 3-chip CCD for surface profiling.

Thus, it makes the measurement faster, simpler and less expensive. As the method requires only one frame, the data acquisition time is only limited by the speed of the CCD camera. The single chip-CCD has three separate spectral bands, R, G, B centered at Red ($\lambda_1 = 620$ nm), Green ($\lambda_2 = 540$ nm), and Blue ($\lambda_3 = 460$ nm) wavelengths respectively. Combining white light interferometer with colour CCD camera allows surface profiling of large discontinuous using a single frame. The theoretical background of Hilbert transformation fringe analysis of colour fringes and experimental results on a micro-specimen are presented.

2. Single fringe analysis using Hilbert transformation

The white light interferogram may be considered as the superposition of the interferograms corresponding to the R, G, B wavelengths. In this procedure we separate the R, G, B data and process them separately. The intensity distribution of any one of the interferograms may be expressed as

$$h_0(x, y) = h_b(x, y) + h_b(x, y)\gamma(x, y) \cos \delta(x, y) \quad (1)$$

where, $h_b(x, y)$ is the bias intensity, $\gamma(x, y)$ is the visibility, and $\delta(x, y)$ is the phase at any point (x, y) in the interferogram corresponding to the wavelength under consideration. In the further discussion the spatial co-ordinates can be ignored for simplicity.

According to the signal theory, a complex wave function $\psi(x) = p(x) + iq(x)$ may associated, with each real wave function $p(x)$. Here, the real part $p(x)$ is the original signal and imaginary part $q(x)$ is the HT of the original signal which is phase shifted by $\pi/2$ [21,22]. Thus MATLAB function 'hilbert' can generate an analytical signal from a real signal. The HT of the signal $\cos(x)$ gives $\sin(x)$, and the HT of the signal $\sin(x)$ gives $-\cos(x)$. In Hilbert transform, only the phases of the spectral components are altered by $\pi/2$, positively or negatively according to the sign of x , but their amplitudes left unchanged [21,22].

Prior to the application of Hilbert transformation, the bias must be eliminated from the signal. If the bias is uniform, it can be removed by applying Hilbert transformation. But the phase analysis in this case requires second time application of HT.

2.1 Fringe pattern with uniform bias

The Hilbert transform of the signal in Eq. (1) can be written as

$$h_1 = \text{Im}[\text{hilbert}\{h_0\}] = h_b \gamma \sin(\delta) \quad (2)$$

where, 'hilbert' is the Hilbert transform function, and Im is the imaginary part of the function. The parameter of interest in Eq. (1) is δ which has information on surface height or depth variations. The signal in Eq. (2) is free from the bias term (h_b) which is eliminated due to HT function. However, Eqs. (1) and (2) cannot be used to evaluate δ correctly due to the presence of bias in Eq. (1).

If we apply HT on Eq. (2) we get

$$h_2 = \text{Im}[\text{hilbert}\{h_1\}] = -h_b \gamma \cos(\delta) \quad (3)$$

Equations (2) and (3) can now be used to give

$$\delta = \arctan\left(\frac{h_1}{-h_2}\right) \quad (4)$$

However, typical white light interference fringes are modulated and associated with non-uniform bias. Such a fringe system can be effectively processed using a min-max method [26,27] as discussed in Section-2.2. The min-max method was proved to be more accurate and intensity variation independent [26].

2.2 Fringe pattern with non-uniform bias

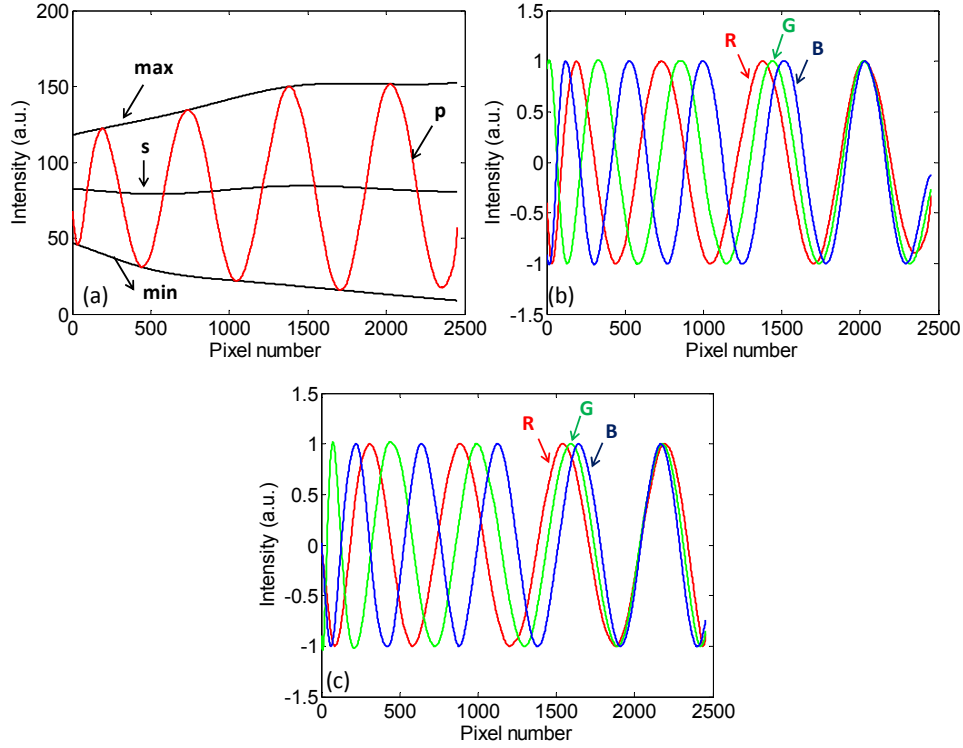


Fig. 1. Eliminating the non-uniform signal bias using min-max method: (a) The original signal-*p*, envelopes of maxima and minima and the mean '*s*', (b) R, G, B components after removing non uniform bias, and (c) HT generated signals corresponding to the signals in Fig. 1(b).

Equation (1) represents a typical signal in the colour channels and may be expressed by as in Fig. 1(a). In the figure '*p*' represents the original signal, *max* and *min* represents the envelopes of maxima and minima respectively. The envelopes are obtained by interpolation in the actual signal. The mean of the two envelopes, $(\text{max} + \text{min})/2$, represents the non-uniform bias and is shown by the curve '*s*' in Fig. 1(a). Equation (1) can be used to obtain $\cos\delta$ at any pixel as [26,27]:

$$\cos(\delta) = \frac{2h_0 - h_{0\text{max}} - h_{0\text{min}}}{h_{0\text{max}} - h_{0\text{min}}} = C \quad (5)$$

Equation (5) represents a cosine signal (*C*). Figure 1(b) represent the signal in the RGB channels obtained in the experiment discussed later.

The HT of the signal in Eq. (5) can be obtained as

$$S = \text{Im}[\text{hilbert}\{C\}] = \sin(\delta) \quad (6)$$

The HT generated signals using Eq. (6) are shown in Fig. 1(c).

Now, the desired phase can be calculated using Eq. (5) and Eq. (6)

$$\delta = \arctan\left(\frac{S}{C}\right) \quad (7)$$

However, the phase δ determined using Eq. (7) differs from the correct argument δ of the cosine function in Eq. (1) because of finite extent of the original signal. HT assumes signals

of infinite extent. Hence the calculated phase using Eq. (7) may be represented as δ' , where δ' may be written as

$$\delta' = \delta + \xi \quad (8)$$

where, ξ is the error. The error due to HT depends on the number of fringe cycles. However, the error ξ can be calculated for any value of δ to create a look-up table which can be used to correct the calculated phase [23,24].

3. Evaluation of the surface profile

The phase δ is related to the surface profile 'z' by the following equation:

$$\delta_i = 4\pi k_i z \quad (9)$$

where, i represents the wavelengths in the RGB channels, z is the height or depth of the surface, $k_i = 1/\lambda_i$ is the wavenumber. The individual phase maps thus evaluated can be used to remove half wavelength ambiguity which appear at single wavelength in two ways: (a) Phase subtraction method [7–9,11], and (b) Fringe order method [12,18,19]. In phase subtraction method, the individual phase values are subtracted to generate phase at an effective wavelength, $\Lambda = \lambda_1\lambda_2/|\lambda_1-\lambda_2|$. This method can extend the unambiguous range, but the resolution of the surface profile measured at an effective wavelength is lowered by (λ/Λ) times [7–9]. On the other hand, the fringe order method can provide surface profile with the resolution of single wavelength and it can extend the measurement range of the single wavelength interferometer [18,19]. In this work, we use fringe order method to achieve ambiguity-free surface profile phase.

The variation of δ_i with k_i is linear as shown in Eq. (9). Using the phases at three wavelengths, it is possible to adjust the wrapped phase data at any pixel such that they lie on a best fit line by addition or subtraction of multiples of 2π . The slope of this line gives the absolute height at the pixel as

$$z_a = \frac{1}{4\pi} \left(\frac{\Delta\delta}{\Delta k} \right) \quad (10)$$

where, $(\Delta\delta/\Delta k)$ is the slope of the line obtained by plotting the individual phases (δ_i) with respect to the corresponding wavenumbers (k_i). The value of z_a obtained from Eq. (11) is less precise but it is quite close to the actual value. The absolute height z_a thus measured can be used to estimate the fringe order (n) using the relation

$$n_i = \text{round} \left(\frac{\delta_i - 4\pi k_i z_a}{2\pi} \right) \quad (11)$$

The function round () gives the nearest integer. Using the fringe order number (n), the total profile height (z) with single wavelength resolution can be obtained as

$$z = \frac{\lambda_i}{4\pi} (\delta_i - 2\pi n_i) \quad (12)$$

Thus the fringe order method allows measurement of large discontinuities and retains the single wavelength resolution of the surface profile.

4. Microscopic white light interferometer

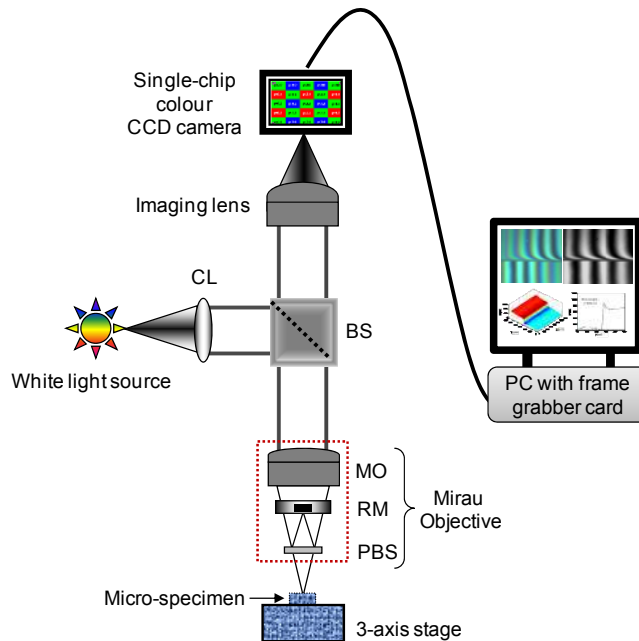


Fig. 2. Schematic of the microscopic white light interferometric system: CL, collimating lens; BS, Beam splitter; MO, Microscopic objective; RM, Reference mirror; PBS, Plate beam splitter.

The schematic of the microscopic white light interferometer shown in Fig. 2 is used for the measurements. A halogen lamp (VISIBLE) is used in the set-up. The white light beam collimated using a lens (CL), illuminates the micro-specimen via the beam splitter (BS) and the Mirau objective. The test specimen is placed on a 3-axis translation stage for alignment. The white light interference pattern generated by the 20X Mirau interferometric objectives is acquired using a high resolution JAI BB-500GE 2/3" GigE vision single-chip CCD camera. The frame rate of the camera is 15 frames per second with full resolution. It is a color progressive scan camera with 5 million pixels resolution and GigE Vision interface. The single-chip CCD camera produces colour images based on a colour filter combination corresponding to the primary colours in which every pixel registers one colour per pixel. The generated colour image has a dimensions 2456(H) X 2058(V) pixels with square shaped pixels of side 3.45 μm . The camera is interfaced to PC with NI PCIe-8231 card from National Instruments (NI). Software programs required for storing and processing of colour white light interferograms are developed based on LABVIEW and MATLAB software packages.

4. Experimental results

Experiments were carried out using the set-up shown in Fig. 2. The test specimen is an etched silicon sample with discontinuities beyond the range of a single wavelength measurement. Figure 3(a) shows the colour image of white light tilt fringes generated on the surface of the test specimen. The dimensions of the raw colour image acquired using the single-chip CCD are 2456 X 2058 X 3 pixels. The colour image is then separated into its individual R, G, and B components of dimensions 2456 (H) X 2058 (V). The decomposed components correspond to Red ($\lambda_1 = 620 \text{ nm}$), Green ($\lambda_2 = 540 \text{ nm}$) and Blue ($\lambda_3 = 460 \text{ nm}$). The signals from the R G B channels are associated with non-uniform bias and are modulated. So, these individual interferograms are processed using min-max method as discussed in Section-2.2. The

interference pattern at λ_1 is shown in Fig. 3(b). The corresponding phase calculated using Eq. (7) is shown in Fig. 3(c). Similarly, the phases at individual wavelengths are calculated using Eq. (7).

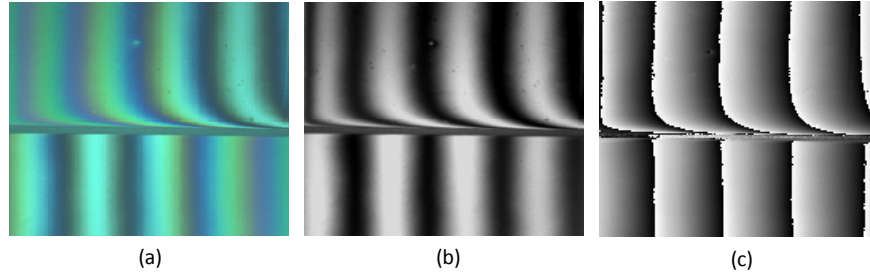


Fig. 3. Fringe analysis using Hilbert transformation: (a) white light interferogram, (b) interferogram at λ_1 , and (c) wrapped phase calculated.

The wrapped phase maps thus evaluated at three wavelengths λ_1 , λ_2 , λ_3 are used to increase the unambiguous range using fringe order method as explained in Section-3. The wrapped phase values at a pixel are adjusted by addition of integers so that the adjusted values lie on a line as shown in Fig. 4(a). The adjusted values are shown by *. The slope of the line gives the absolute value of z at the pixel. Figure 4(b) shows the ambiguity removed 3-D surface profile using the fringe order method for $\lambda_1 = 620$ nm. The surface profile measured along central y -axis is shown in Fig. 4(c) and as expected it has the usual smoothness of single wavelength phase shifting interferometer. The height of the step has been determined by linear least square fitting across the top and bottom of the profile (Fig. 4(c)) and determining the height difference at the location of the step. From the analysis, the step height value measured is 645 nm. Only, the 3-D surface of an etched silicon sample reconstructed at λ_1 is shown in Fig. 4(b). However, all the three combinations (n_1, λ_1) , (n_2, λ_2) , and (n_3, λ_3) in Eq. (12) will generate the same profile height depending on the accuracy of the central wavelength of the R, G, B channels of the colour camera.

The proposed HT method can be used for optical inspection of microsystems such as MEMS, micro-lens array, AFM cantilever, etc. It requires only one frame; hence it can be used for dynamic interferometric measurements as well. The repeatability of HT method is expected to be at least as good as phase shifting method, as only one frame needs to be taken, and instrumentation is less. We found that the HT method can generate the phase map ~ 4 times faster than the 8-step phase shifting method. The application of HT on an open fringe system (such as tilt fringes) is straight forward. If the object generates closed fringes, 1-D HT will introduce an ambiguity in the phase map. However, it can be solved by following the procedures discussed in the References [23–25]. The maximum measurable step height depends on the coherence length in the three channels. For the camera used, the filters in the three channels are relatively broad (~ 70 nm), and coherence length is estimated to be about 4 μm . The choice of the wavelengths is governed by the filters in the three channels of the CCD.

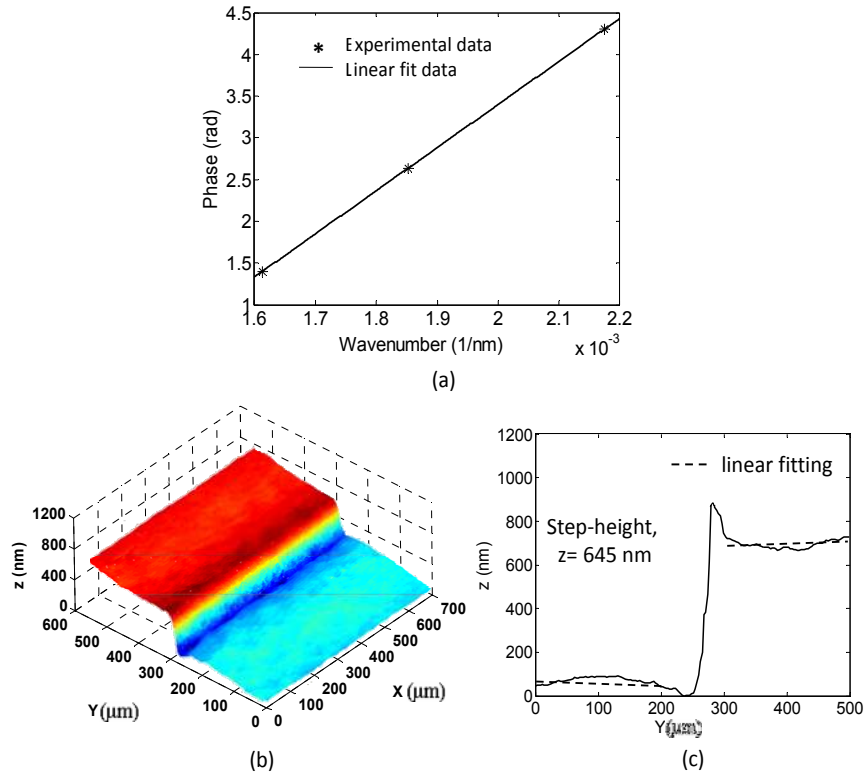


Fig. 4. Surface profile analysis using the fringe order method: (a) The linear fitting of the adjusted phase values measured at three wavelengths at a given pixel, (b) 2π ambiguity corrected single wavelength 3-D surface profile of an etched silicon sample using the phase at λ_1 , and (c) line scan profile showing the step height 645 nm.

5. Conclusions

We have demonstrated the procedure to obtain ambiguity free step-height measurement using single white light interferogram acquired using a single-chip colour CCD camera. White light interferogram, stored using the color CCD, is decomposed in to individual R, G, B components. A phase shifted frame is obtained using Hilbert Transformation. The error introduced due to the HT of finite length signal is corrected by look-up tables. The need for phase shifting hardware is avoided making the process simpler and faster for industrial applications.

Acknowledgment

The authors acknowledge the financial support of the University Start-up Grant at Nanyang Technological University.